IEEE Access
Multidisciplinary : Rapid Review : Open Access Journal

Received December 23, 2021, accepted January 5, 2022, date of publication January 11, 2022, date of current version January 18, 2022.

Digital Object Identifier 10.1109/ACCESS.2022.3141981

The Effects of Torque Magnitude and Stiffness in Arm Guidance Through Joint Torque Feedback

HUBERT KIM AND ALAN T. ASBECK
Mechanical Engineering Department, Virginia Polytechnic Institute and State University, Blacksburg, VA 24061, USA
Corresponding author: Alan T. Asbeck (aasbeck@vt.edu)

Hubert Kim was supported by a Virginia Tech Institute for Critical Technology and Applied Science Doctoral Scholars Fellowship. This work was also supported by a Google Faculty Research Award, and its publication was supported by the Virginia Tech Open Access Subvention Fund.

This work involved human subjects or animals in its research. Approval of all ethical and experimental procedures and protocols was granted by the Virginia Tech Institutional Review Board under Approval No. IRB #16-175.

ABSTRACT Joint torque feedback is a new and intuitive way of delivering kinesthetic feedback to a person or guiding them during motion tasks via wearable devices. In this study, we performed three experiments to understand how the elbow joint responds to guidance via small torques (< 1 Nm). We first applied open-loop torque pulses to the elbow, and determined the magnitude and delay of the resulting arm motion. Second, we provided pulses of a desired position trajectory in combination with a torque proportional to the error between the joint's angle and the target angle. We compared the effects of different ratios between the error and applied torque, which is the torque stiffness. Finally, we investigated step inputs from one angle to another in conjunction with different torque stiffnesses. We found that open-loop extensional torques caused large elbow movements, independent of the torque magnitude or duration, while flexional torques caused arm motion proportional to both the magnitude and duration. With position pulses, the highest gain of 0.095 Nm/deg resulted in mean position errors of less than 10 degrees, while the lowest gain of 0.012 Nm/deg resulted in mean position errors of nearly 20 degrees. The higher gains caused the arm to move faster and required higher torques, likely due to masking. The arm had a bandwidth of close to 2 Hz, and step inputs resulted in larger mean errors during flexional motion (15.3 degrees for flexion vs. 9.0 degrees for extension).

INDEX TERMS Haptic feedback, motion training, physical human-robot interaction, virtual wall, joint torque feedback.

I. INTRODUCTION

Haptic feedback has been a traditionally effective means for delivering training in movement sequences. Frequently, this has been accomplished through tactile feedback, using the sense of touch to convey information to a person. Tactile feedback is beneficial for its design flexibility as the actuators are typically small and easy to construct. For example, Bark *et al.* fabricated a wearable robot made of four vibrotactile motors and explored one to four degrees of freedom arm motions [1]. Skin stretch was also tested for supplementing spatial perception [2], and mechanotactile feedback (brushing against the skin and tapping on the skin) was investigated as a means of replacing proprioceptive perception for arm amputees [3], [4].

The associate editor coordinating the review of this manuscript and approving it for publication was Pedro Neto.

An alternative to tactile feedback is kinesthetic feedback, conveying information to a person through the limb positions and forces on the muscles. This has the advantage of being an intuitive method of feedback, as people already detect their limb positions and forces during motions. Some researchers have investigated kinesthetic feedback through a manipulandum display for training tennis motions [8] and rowing training [9]. Another type of kinesthetic feedback is joint torque feedback (JTF): JTF is feedback delivered by a wearable device that creates a small torque around a joint to guide the wearer's motion, similar to how a physical trainer might guide a person's limb during rehabilitation or motion training. JTF is distinctive from other methods of tactile feedback because the stimulated sensory organs are the same proprioceptors used for body coordination. For example, Carignan *et al.* utilized a multi-joint system [10] of JTF to display a virtual wall during a wall-painting task. Thomas *et al.* adopted both JTF and vibrotactile

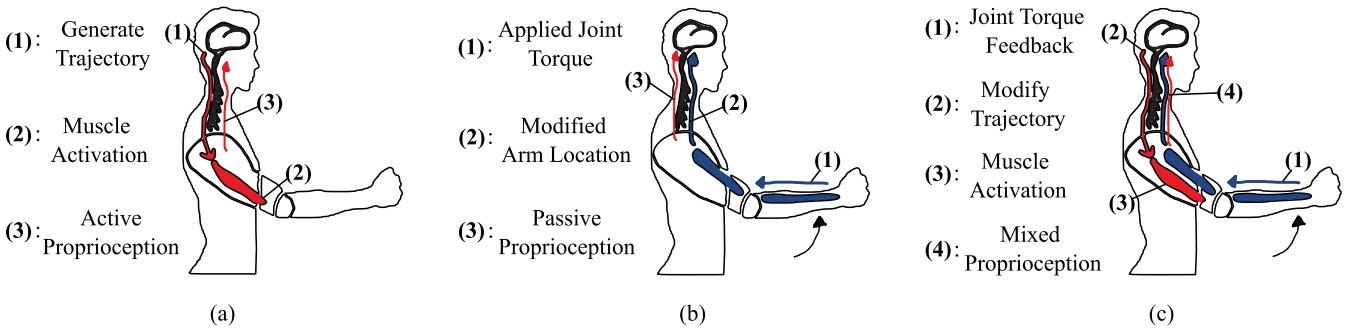

FIGURE 1. Conceptual diagram showing the different types of proprioception [5], [6] and its role in arm movement control [7]. (a) Obtained/Active proprioception. (b) Imposed/Passive proprioception. (c) Mixed proprioception.

feedback to convey information about the stiffness of objects [11].

Since JTF uses the same sensory organs as used during volitional motions, it is useful to discuss the neural pathways involved in motion and sensory feedback. Proprioceptive feedback can be classified into two types, obtained and imposed proprioception [6]. Obtained proprioception (also referred to as active proprioception) is the body sensation realized by active movement, where the fusimotor neurons and joint receptors provide feedback to the brain (Figure 1(a)). Obtained proprioception is initiated with an afferent nervous pathway, the motor command from the Central Nervous System (CNS) to muscle groups (Figure 1(a-1)). Traditionally, this is experimentally investigated by asking a subject to move their limb to a certain position without seeing it [12]–[14]. In comparison, imposed proprioception occurs when the body segment is externally driven (Figure 1(b)). In this case, proprioceptive stimuli delivered to the CNS (efferent nervous pathway) trigger proprioception. When an external force moves a limb, the skin receptors around the joint are known to be the principal source of measurement [15], [16]. Experiments were conducted on blindfolded subjects who notified the experimenter when they detected the passively-driven motion [17]–[19]. Similarly, in a contralateral kinesthetic tracking test, subjects were instructed to move their right arms according to the angle change of the left elbow [20].

Physically guiding a limb via a wearable display, such as with JTF, requires both active and passive proprioception, as illustrated in Figure 1(c). In this scenario, physical guidance triggers the wearer's movement (efferent pathway) while individuals still follow the guidance (afferent pathway). It is this scenario that we explore in this paper—where JTF is provided to a person while they are moving, in order to help guide their motion.

Some studies have addressed the case when both obtained proprioception and imposed proprioception occurred together. In order to study different perception delays between the obtained and imposed proprioception, Chapman *et al.* applied electrical stimulation to the index finger skin before and after the elbow extension, comparing the case when the arm was actively moved or passively driven [21]. The user response yielded a 38 ms longer delay when subjects actively moved their elbow compared to when it was passively driven; this observation indicates that the afferent signal of actuating the elbow possibly affects efferent perception of tactile stimuli, resulting in the delay in the sensation. While an afferent motor command leads to a delay in perception, both active and passive movement have been observed to affect perceptual ability through masking. The masking effect of the movement over the efferent nervous pathway has been defined as backward masking [21]–[23]. From observing individuals responding to an electric stimulus on the right extensor carpi ulnaris, Collins *et al.* found that the passive and active movement was responsible for 37-40% of velocity-dependent attenuation of the muscular sensation [22].

Obtained and imposed proprioception can also occur together if a person is being guided with a manipulandum (an object such as a handle that is being moved). However, JTF is distinct from the kinesthesis (i.e., perception of body movements) that results from manipulandum devices. Gillespie *et al.* argued that the forces provided through a manipulandum are delivered to the trainees as the combination of the manipulandum's dynamics (forces and motions due to its inertia, kinematic constraints, external forces, etc.) and desired behavior (forces and motions displayed through the manipulandum to the trainee), and people might find it challenging to differentiate the two [24]. Even from a physiological perspective, proprioception felt via an end-effector takes place with multiple haptic sensory organs. For example, measuring force feedback on the arm's elbow through a Phantom Omni device accompanies tactile sensors on the palm, joint receptors on the wrist, and elbow [25]. In contrast, JTF typically uses a single direct-drive actuator per joint degree of freedom [10], [11], [26], [27].

In a motion guidance task with JTF, torques are given to a person's joint so that the person moves the joint through a desired kinematic trajectory. One method of doing this is to provide a joint torque τ_{JTF} that is proportional to the angular error θ_{error} between the joint's actual position and the desired position. For a given angular error, there might be a small joint torque or a large joint torque. The torque stiffness is defined as the change in applied torque $\Delta\tau_{JTF}$ per change in angular error, i.e., $k = \Delta\tau_{JTF}/\Delta\theta_{error}$. Figure 2 illustrates

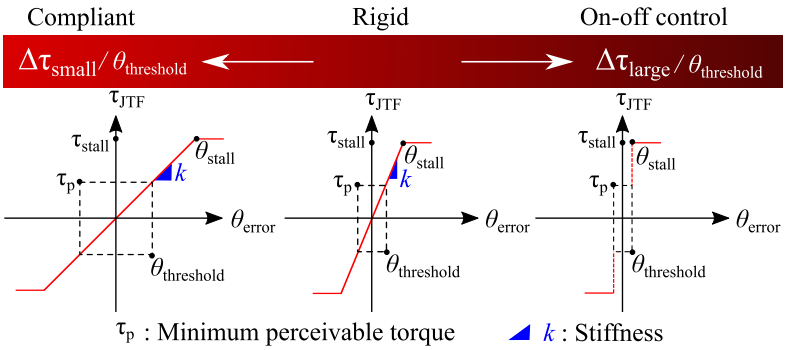

FIGURE 2. **During arm guidance, an exoskeleton provides a joint torque τ_{JTF} as a function of the error θ_{error} between the desired and actual arm angle. This diagram presents several options for the function relating the error and applied torque. The torque stiffness, $k = \Delta\tau/\Delta\theta_{error}$, is small on the left and large on the right. Three example stiffness levels are shown: left, Compliant JTF has a shallow torque slope, and the JTF provides cues but does not hinder the arm's motion. Center, Rigid JTF has a steep torque slope, such that the JTF may constrain the wearer's arm or cause it to move. Right, On-off control JTF has a vertical torque slope, where JTF delivers a binary (on-off) cue. τ_{stall} is the torque limit due to the hardware limit; τ_p is the smallest perceivable torque; θ_{stall} is the position threshold where the provided JTF becomes τ_{stall}; and $\theta_{threshold}$ is the position threshold where the JTF becomes τ_p.**

this idea of torque stiffness in motion guidance. The top of the figure shows a continuum of possible torque stiffnesses: at the left, very compliant feedback has a small applied torque for a given error. At the right (on-off control), very stiff feedback will provide some maximum amount of torque for even small angular errors.

The bottom of the figure shows the continuum of torque stiffness more quantitatively. Three graphs show the applied torque as a function of the angular error with a red line. Each graph also shows several key points: τ_p is the minimum perceivable torque; $\theta_{threshold}$ is the angle that corresponds to this minimum perceivable torque; τ_{stall} is the maximum output torque from the actuator, which may be larger or smaller than the maximum biological torque that the joint is able to produce; and θ_{stall}, the angle that corresponds to this maximum (stall) torque.

The three graphs illustrate examples of the torque stiffness continuum as indicated at the top of the figure. At the left, in Compliant feedback, the JTF will ultimately be larger than the minimum perceivable torque τ_p, but since the torque stiffness is low, a large angular error is required before the feedback is perceivable. In this case, the JTF is unlikely to disturb the arm motion because a very large angular error is required before the applied torque is strong. Thus, JTF works as both an event cue (informing the person if they are deviating from the path, when the perceptual threshold is crossed) and additionally provides information about the spatial error, since the provided torque is proportional to the error. This level of torque controller is likely appropriate for a patient-driven control strategy [28]. In the center, with Rigid feedback, the angular error before the torque is perceivable ($\theta_{threshold}$) is much smaller because the torque stiffness is larger. This also may be useful for a patient-driven control strategy depending on the specific slope. Finally, at the far right, On-off control corresponds to the person feeling corrective torques in one or the other direction almost all the time, modulated only by the angular error at which the torques begin ($\theta_{threshold}$) and the compliance of the human interface between the person and device providing JTF. Tan *et al.* [29] found that a linear stiffness of 24.2 N/mm was required to be perceived like a rigid wall when vision was blocked. Later, [30] further developed the perception of virtual stiffness with a stylus-based approach and found that the maximum distinguishable stiffness was as small as 0.3-0.4 N/mm. At this level, θ_{stall} becomes almost $\theta_{threshold}$.

At first glance at Figure 2, it seems evident that applying a higher gain would lead to better tracking. However, a closer examination reveals that simply increasing the stiffness does not necessarily lead to better performance in a human learning a motion trajectory. According to the guidance hypothesis, the corrective cues derived from a position error can be helpful yet the person should not be dependent on them for guidance [31]. Excessive guidance without considering the human perceptual level could dominate the subject's perceptual ability, and there is little autonomy left for the wearer to play any role in tracking [31]–[33]. This argument is in agreement with the observations from [8] and [9] where a position controller yielded better tracking accuracy than a path controller, yet degraded the participants' self-initiation of motion. Moreover, prior experiments have found that proprioceptors have a velocity-dependent or muscle contraction-dependent Weber fraction [25], [27], [34], [35]. The stronger a muscle is isometrically contracted, the worse the perceptual resolution becomes, and the faster a joint moves, the worse the perception ability [34].

Another consideration with respect to torque stiffness is whether or not the JTF could move the arm due to the applied torque or otherwise impede the person's motion. The torque required to move a relaxed arm varies from 1 Nm/rad to 4 Nm/rad, depending on the joint conditions [36]. Though

we cannot completely decouple the arm's motion due to JTF and the person's voluntary movement, we expect to observe that keeping the JTF magnitude close to the perceptual level (i.e., close to the just-noticeable level) will not hinder the arm movement. Referring to Figure 2, the magnitude of τ_{stall} can lead to different sensations of JTF for any of the three cases shown. If τ_{stall} is only slightly larger than τ_p, then the JTF functions only as an event cue: it only tells the discrete information of if the arm is following the trajectory correctly or not, as well as the direction of the error, but does not provide any information about the magnitude of the error. In this case, there is a "deadband" where the user cannot feel anything at all until their angular error exceeds $\theta_{threshold}$. This deadband could be very narrow or wide depending on the torque slope. Also, since the maximum feedback torque is so small, the wearer's joint is free to move without interference from the feedback system.

In comparison, if τ_{stall} is very large, then above some angular error the user's arm will be forced to follow the commanded trajectory. With a high torque stiffness, this happens with small angular errors, leading to a discrete-like JTF where the $\theta_{threshold}$ becomes θ_{stall} (shown at the far right of the figure).

Our pilot test found that an on-off controller made of JTF with a Just Noticeable Difference (JND) level of stall torque could not provide sufficient information to the subjects to follow a desired trajectory. When the position threshold at which the torque was provided was set to be small, the exoskeleton was unstable and constantly changed the direction of the torque. Even when there was a larger position threshold, the subject could not tell how much their joint should move.

However, with a moderate or small torque stiffness, the user will receive input on both the direction of motion and the magnitude of their error. For the JTF to be utilized as haptic guidance, it should deliver "when to move," and "how much travel" regardless of the wearer's joint condition [37]. Therefore, the maximum torque amplitude provided by JTF (τ_{stall}) is suggested to be closer to the JND level, with just enough amount of torque to be noticeable but not disturb the motion, and the torque stiffness should potentially be a low or moderate value to maximize information transfer to a user.

In this paper, we investigate specifically how people respond to joint torque feedback, with the goal of better understanding how it can be used for motion training or otherwise used to convey information to a person. We study the JTF perception in three different ways:

First, we examine how people move their arms with different magnitudes and durations of a pulse of torque, referred to as a Current Pulse (CP). A pure torque pulse is applied to the elbow, and the user moves in response to the torque. With this, we determine how a person responds to different pulse magnitudes and durations. This also allows us to investigate if the previously measured JND torque at the elbow is strong enough to guide the arm [27], [34]. Second, using the framework in Figure 2, different torque stiffnesses ranging from Compliant to Rigid are studied with a Position Pulse (PP). A nominal position trajectory in the shape of a pulse is provided to the elbow, in conjunction with JTF with various torque stiffnesses. Different amplitudes and durations of the position pulse are investigated. The JTF implemented in this study is limited to about 1 Nm, which is not nearly strong enough to constrain the arm to a target trajectory. Accordingly, the user's arm dynamics and perceptual ability are the two critical elements in determining the tracking performance. These pulses are examples of JTF being used to guide a motion without interference with voluntary arm movement, promoting use-dependent plasticity. Third, we explore how the joint's physiological condition affects the wearer's perception when tracking a Position Step (PS). A commanded step input from one joint angle to another is provided to the elbow, in conjunction with one of two possible torque stiffnesses. From Latash *et al.*'s review, the human joint has inherent stiffness that varies depending on the angle [36]. Thus, even the same magnitude of JTF may lead to a different final angle when the initial angle is different. In this experiment, we investigate how the initial and final arm angles affect the tracking performance.

II. MATERIALS AND METHODS

A. MATERIALS

1) HARDWARE

A right-arm exoskeleton made of an aluminum frame wrapped around a plastic cuff and actuated by a brushless DC (BLDC) motor (Antigravity MN7005 KV115, 24N 28P) was used to provide JTF (Figure 3(a)). This same exoskeleton was used in our prior studies [26], [27], [34]. To operate the motor, a Texas Instruments (TI) C2000 TMS320F28069M microcontroller with the TI DRV8305 motor shield was used. The maximum operating current limit was set to 14.4 A, which is nearly the motor shield's maximum allowable current of 15 A. The exoskeleton is designed to mask the sensation of pressure over the arm by squeezing tightly against the arm with at least 0.015 N/cm^2 [29]; this prevents the participant from noticing the exoskeleton pushing on the arm when it moves. The internal pressure is measured with four FSR sensors (size: 4.5 × 4.5 cm) when donning the exoskeleton. In addition to the exoskeleton, a computer screen and speaker provided visual direction and sound cues. Figure 3(c) shows the Graphical User Interface (GUI) on the screen. The FSR readings are displayed on the top right corner of the screen as four red circles. When the pressure reading becomes more than the threshold, the circle turns green. We used MotorWare's built-in electrical angle module instead of the custom electrical angle estimation feature from [26] to improve the BLDC motor's stability. A custom testbed fixture was built to hold the upper arm 45° with respect to vertical (Figure 3(b)). Rather than initiating the arm movement from full flexion, the inclined reference position accounts for the possible misalignment between the exoskeleton and the various arm geometries. Thus, the range of motion is designed to be 45±45°. The torque constant of the motor, 0.072 Nm/A,

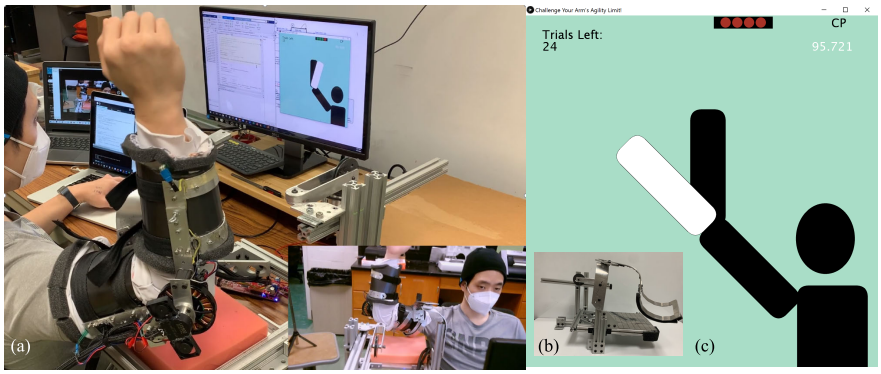

FIGURE 3. (a) A subject participating the test. (b) The aluminum test setup for holding the arm 45° inclined. (c) A sample GUI for the demonstration. The white arm indicates the participant's arm position while the black arm guides the desired arm motion. The black arm is not present once the test begins.

used to detect the applied torques in conjunction with the current, was calibrated with a FUTEK LBB200 load cell with a Tacuna Systems Amplifier v.2.3.

2) SOFTWARE

Three software platforms were implemented. Processing 3.0 was used for realizing the GUI, Texas Instruments Code Composer Studio (CCS) was used for reading sensors and actuating the motor, and MATLAB was used for processing the results.

The randomized experiment pairs for different subject groups were defined in Processing 3.0. Upon executing, the software loaded all the predefined segments of path files into object arrays. Then, the internal state machine transmitted each position input in a random order to CCS. The GUI system realized with Processing is run at 100 Hz while data logging speed was 200 Hz based on the SCI communication between Processing and CCS. Next, CCS sent the position input to the microcontroller. MATLAB processed the received data from Processing and presented the tracking performance. After each trial was conducted, the visualized results were provided via MATLAB.

The position error-driven controller (PD controller) with different gain conditions was defined in CCS (Figure 4). With the implemented PD controller, the torque stiffness is only controlled with the proportional gain. The damping term is only tuned once without the human arm. Hence, the corrective effort suitable for JND is evaluated by the torque slope or the Proportional gain.

We chose four different levels of torque stiffness, illustrated in Figure 4. Gain One (G1) is a shallow gain with 0.012 Nm/deg; Gain Two (G2) is a steep gain of 0.038 Nm/deg; Gain Mixed (GM) is a combination of G1 and G2; Gain Three (G3) is the closest to a virtual wall, with 0.095 Nm/deg. Referring to Figure 4, the slope is steepest to shallowest in the order of G3, G2, GM, and G1. For each gain, the figure also shows the position θ_{stall} that defines the boundary where proportional spatial information can be delivered: any position error beyond this boundary corresponds to the motor providing a fixed maximum stall

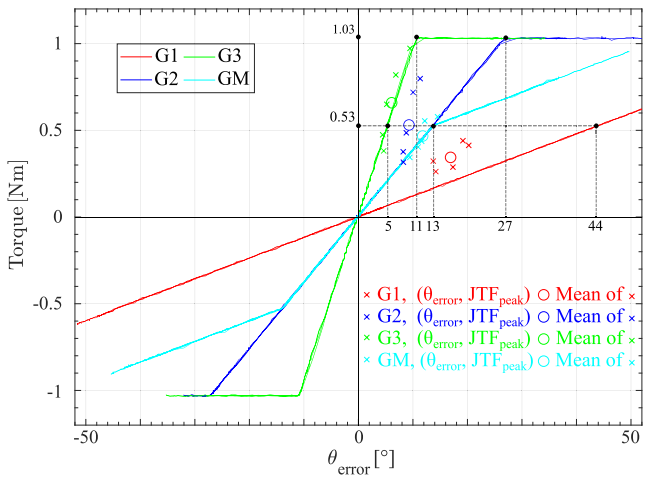

FIGURE 4. Four different levels of torque stiffness. Dashed lines represent the position that corresponds to a torque of 0.53 Nm for comparison. Also, vertical black dotted lines indicate θ_{stall}. Shown are Gain One (G1, shallow gain-0.012 Nm/deg); Gain Two (G2, steep gain-0.038 Nm/deg); and Gain Three (G3, virtual wall-0.095 mNm/deg). The mixed gain GM is designed to have the same torque slope as G1, with an offset of 30°. Positive position errors indicate flexional arm displacement; negative errors are extensional arm motion. τ_{stall} is the system's peak torque, which is 1.03 Nm. Within the figure, small ×s indicate results of the mean error θ_{error} and peak feedback torque during the Position Pulse experiment (data from Figure 9); ○s are the means of the same-colored ×s. Typically, higher-frequency pulses (i.e. with shorter durations) had larger peak torques.

torque τ_{stall}. The values of θ_{stall} for the different conditions, from smallest to largest, are in the order G1, GM, G2, G3.

From pilot testing, we found that when θ_{stall} became smaller than 10°, it caused an unstable feedback system to the wearer by constantly switching the direction of the torque. Therefore, when sizing the shallow torque slope (G1), we used the smallest position threshold (10°) in conjunction with the converged JND torque value from our prior study with the arm at rest, which is around 0.10 − 0.14 Nm [27], [34]. The G1 slope passes close to this point. The G3 is the maximum torque slope that was achieved for our hardware setting. In this case, we chose the slope so that the maximum torque provided by our exoskeleton (1.03 Nm) occurred with close to 10° of position error.

The positions before reaching the stall torque for each gain condition (θ_{stall}) are 87°, 55°, 27°, and 11° for G1, GM, G2, and G3. The GM level was specifically implemented to investigate whether a change of slope could affect the tracking accuracy. Specifically, we used a steeper slope (matching G2) at small position errors, followed by a shallower slope (matching G1) for high position errors. These two slopes connected around the breakpoint of 0.5 Nm and 13° (Figure 4), which is around 30° less than where the G1 slope crosses 0.5 Nm. With this offset, we hypothesized that the GM slope would yield about a 30° more accurate result than the G1 slope for situations in which high torques (> 0.5 Nm) were needed.

Again referring to Figure 2, we consider the torque slope and the position threshold relative to the perceptual threshold, τ_p, which is $0.10-0.14$ Nm when the arm is at rest according to our prior studies [27], [34]. The corresponding position thresholds ($\theta_{threshold}$) are 1, 3, and 10° for G3, G2, and G1, respectively. These range from quite small (G3) to relatively large (G1), allowing us to understand a range of conditions.

B. METHODS

1) PARTICIPANTS

We recruited 15 subjects, 13 male and 2 female, ages 29.31 ± 4.00 years, who were all healthy right-handed participants. The experiment was reviewed by the Human Research Protection Program at Virginia Tech for the COVID-19 mitigation process and approved by the Virginia Tech Institutional Review Board (IRB #16-175).

All participants were informed about the COVID-19 safety guidelines along with the study's goal. The individuals were instructed to not entirely relax their arm during the test, and to pay attention to how they felt on their right arm. Also, they were asked not to wiggle their arm when they were not sure about whether the force was applied or not. Some subjects with thin arms had additional padding foam inside the exoskeleton cuffs.

Subjects were randomly assigned to two groups, Position Step or Position Pulse. Both groups first participated in the Current Pulse test, followed by either Position Step or Position Pulse, depending on the assigned group. The test took about 45 minutes (10 minutes of Current Pulse, 30 minutes of Position Pulse or Position Step, with 12 minutes (4 times 3 minutes) of breaks between sessions). A demonstration trial preceded each session. A small amount of monetary compensation was provided for participation.

2) PRE-PROGRAMMED INPUT

To study the human response to open-loop torques (Current Pulse) and desired positions in conjunction with a torque stiffness (Position Pulse), we used a single smooth pulse input shape, where we could alter the magnitude and duration. The pulse for both of these tests was characterized by a raised cosine function with the roll-off factor of 0.5 and limited to positive values:

$$Torque = \max\left(\left(\frac{sin(\pi t/T)}{\pi t/T}\right)\left(\frac{\cos(0.5\pi t/T)}{1-(t/T)^2}\right),\ 0\right)$$

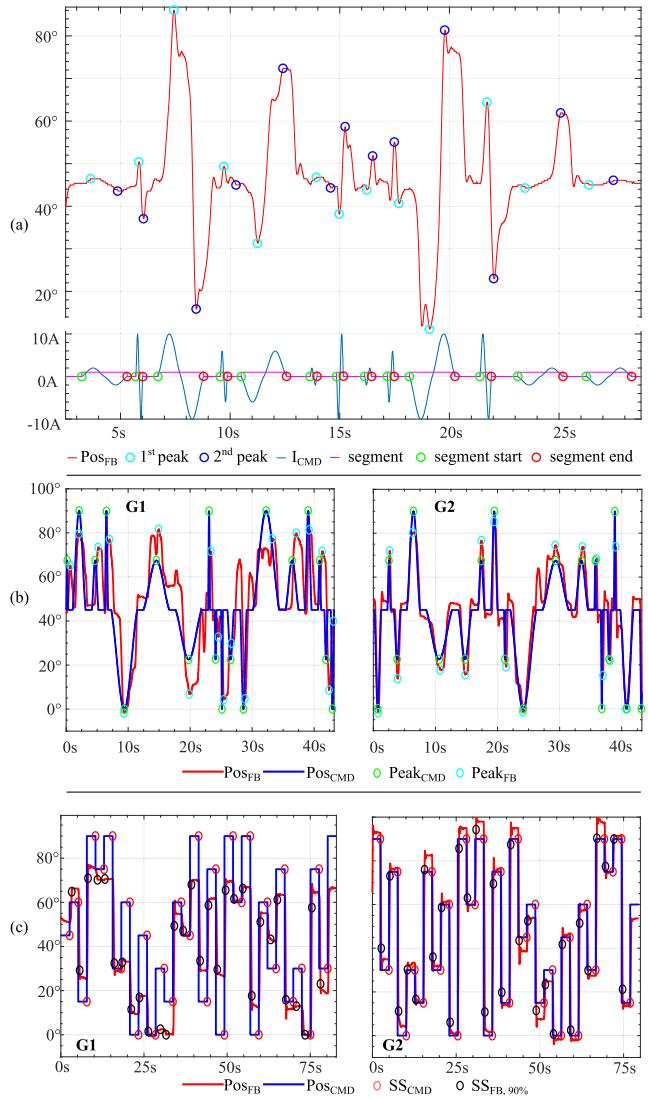

FIGURE 5. Sample test results showing how piece-wise analysis is conducted. Blue is the commanded input, and Red is the wearer's arm movement. The three types of input are shown in different subfigures. (a) Current Pulse. Magenta is the segment; green and red circles show the beginning and ending points; cyan and blue circle indicate first and second peaks. (b) Position Pulse. Green and cyan circles are commanded position peak and arm movement peak. (c) Position Step. The red circle is the steady-state commanded position; the Black circle illustrates 90 % of the arm's steady-state position. The positive direction illustrates the arm flexional motion; negative y-values show arm extension movement.

where *Torque* is the torque applied, t is time, and T is the period. With $T = 1$, this results in a pulse shape from $t = -1$ to $+1$, with a maximum amplitude of 1 at $t = 0$. A single waveform was generated in this manner and then scaled to match the amplitudes and durations for each condition. Unlike the Position Pulse which was applied as a single pulse, the Current Pulse was applied as a pair of either positive-negative or negative-positive waves (Figure 5) so that the person's arm would stop moving and return toward its starting position after each initial pulse.

The programmed state machine in Processing 3.0 randomly selects the base magnitude and duration. Lastly, the system resizes the original input array and presents the

stimulus to the participant. The specific details of each test are as follows:

Current Pulse (CP): The chosen magnitude for the CP involves 2, 6, and 10 A, which corresponds to torques of 0.144, 0.432, and 0.72 Nm. The durations were chosen from $\{0.3, 0.5, 1, 2\}$ seconds (which we plot as $\{3.3, 2, 1, 0.5\}$ Hz), leading to twelve input combinations. However, we applied two pulses consecutively in opposite directions as a pair. Therefore, the CP state machine randomly chooses the combination of one of the three magnitudes; and one of the four durations, each of which has both a positive-negative and negative-positive pair (8 options). Figure 5(a) shows a sample CP input (bottom plot) and subject's response (top plot).

Position Pulse (PP): We created pulse signals from five different durations ($\{0.6, 1, 2, 4, 8\}$ seconds, corresponding to frequencies of $\{1.67, 1, 0.5, 0.25, 0.125\}$ Hz) with the magnitudes of $\pm 22.5°$ and $\pm 45°$. The generated pulses are played in a random order. The state machine programmed in Processing randomly chooses the magnitude and the duration at every trial until all combinations of pairs are finished. It always started at 45°, going to a peak angle of either 67.5° or 90°. To mitigate human guessing, the system also adds or subtracts a small amount of magnitude $(0 - 10°)$ from the peak. Next, the input always goes back to 45° so the arm can return to a fixed position at the beginning of each trial. Thus, we compare the four different perceptual conditions, assuming that the arm responds similarly in terms of its range of motion. The time in between each pulse is 2 seconds. Figure 5(b) shows an example input and subject's response for the Position Pulse test, with two gains shown.

Position Step (PS): When transmitting step inputs, the position data sent to the motor shield passes through a first-order Low Pass Filter with a rise time of 0.5 seconds. Then each segment of input lasts 5 seconds. The initial and final angles are selected from $\{0°, 15°, 30°, 45°, 60°, 75°\}$. Based on our pilot test, we eliminated some combinations where the input is sometimes too small for the wearer to perceive it as well as several others to reduce the total experiment time. The excluded pairs are: 0° to 15°, 15° to 45°, 30° to 45°, 45° to 75°, and 60° to 75° for increasing steps; and 15° to 0°, 45° to 15°, 45° to 30°, 75° to 45°, and 75° to 60° for decreasing steps. Figure 5(c) shows a sample Position Step result, including the commanded position trajectory and the subject's response for two different gains.

3) EXPERIMENTAL PROTOCOL

The experiment was carried out in two groups, one group with Current Pulse then Position Pulse and another with Current Pulse then Position Step. For both groups, the Current Pulse was tested before the other experiment. Also, a tutorial session preceded each session. The tutorial's goal was to provide the correct answer such that the participant could understand the experiment and receive a small amount of feedback about their behavior's result. The results shown on the screen during the tutorial were the visualized individual's arm and desired location, the average time delay, and their position error.

The break time in between the sessions was selected to be at least 5 minutes. During the break, the motor is powered off, and the subjects were allowed to take off the exoskeleton and relax their arm.

Amid the break between sessions, the individual's tracking result of the previous trial was displayed on the screen. The screen included the exoskeleton's desired path and the participant's arm movement. The report was introduced to motivate and facilitate the participant's engagement, similar to "attention check" sections in a psychological survey. Since the proprioception is a result of physiological and psychological efforts [6], paying attention throughout the experiment played a key role.

The following experimental procedures were applied to all three experiments: The test started with the experimenter helping the participant put on the exoskeleton. When donning the exoskeleton, the subjects' elbow was aligned with the motor. Also, to mitigate the tilting of the shoulder and unexpected fatigue, individuals were asked to sit as close as possible to the aluminum pad. The participant's arm was fully extended and supinated when tightening the straps. Next, the participant changed their posture to be in a comfortable position. The experimenter adapted the sitting height and the platform's location based on the arm's volume and weight. Then, the tester ran the GUI system and enabled the CCS script. Finally, the exoskeleton calibrated via the index pin to reset the encoder, and data logging began. For both Position Step and Position Pulse, the initial arm angle is 45 degrees inclined from the desk to minimize the gravity effect near the reference angle. However, some subjects with a long upper arm length tended to incline too much toward the desk and the arm support platform had to be adjusted accordingly. Finally, the GUI setup and required rules were explained to the subjects before the practice session. During the practice session, subjects were allowed to move their arm back and forth to feel the sensation of being driven by the exoskeleton. However, they were asked not to be hesitant or conduct exploratory motions during the actual sessions.

During the Current Pulse trials, subjects could not tell when the input execution process was finished because the end of the second torque pulse was difficult to detect. In general, the torque pulses frequently led to the arm moving with a net displacement away from the starting position. Therefore, a beep sound was introduced to cue subjects when the exoskeleton finished applying torque in both directions. Upon the beeping sound, subjects were asked to move their arm back to the neutral position. The experimenter confirmed that the arm was at the neutral position before proceeding to the subsequent trial.

The experiment was conducted in an empty space apart from the participant and the experimenter. During the tracking, subjects were allowed to close their eyes for better concentration except for the practice session, which provided visual information to the subject.

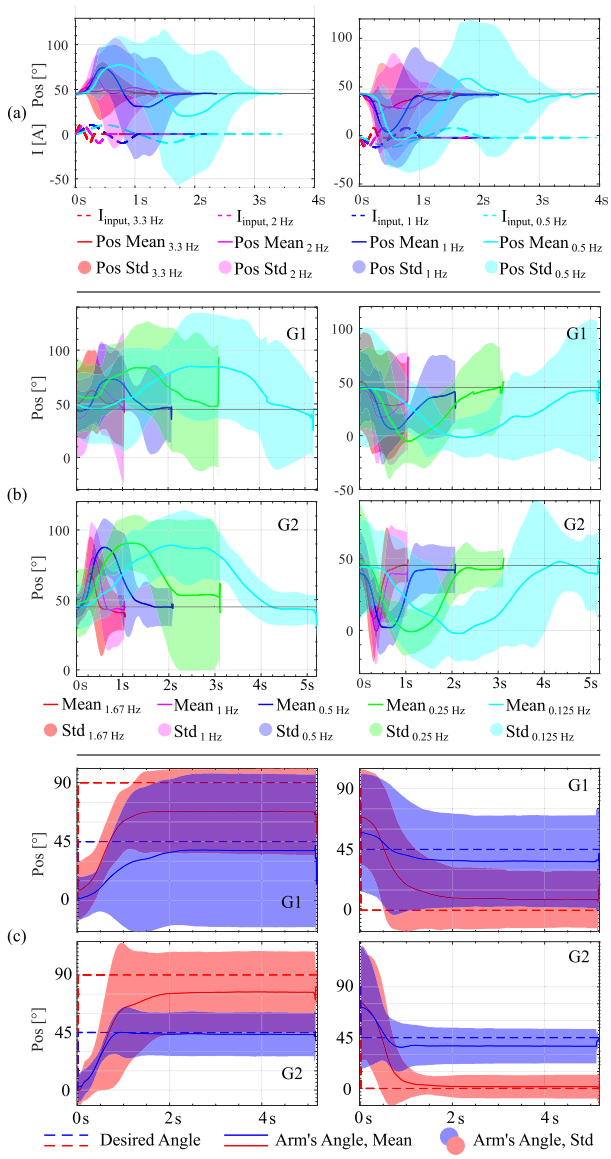

FIGURE 6. Test results for several examples of each type of test. In each plot, the solid line is the mean arm angle as a function of time, and the shaded area is the standard deviation. The positive y-axis is the flexional direction, and negative y-axis the extension direction. (a): Current Pulse result of 10 A magnitude with 0.3, 0.5, 1, and 2 seconds of duration. The dashed line shows the applied current. (b): Position Pulse results for 45° Pulse Input with 0.6, 1, 2, 4, and 8 seconds of duration. (c): Step response of increasing angle from 0 to 45° and 0 to 90° and decreasing angle from 90 to 45° and 90 to 0°. The dashed line shows the commanded step input.

III. RESULTS

For each session, the continuous time-domain data (Figure 5) was segmented into each trial and aligned (Figure 6) via MATLAB. The test data was analyzed as a repeated measures design. The p-value from the Repeated Measures ANOVA (RMANOVA) was corrected with the false discovery rate (FDR) method to account for multiple hypothesis testing. Pairwise comparisons were made with Tukey post-hoc tests. Statistical analysis was performed with JMP Pro 15 (SAS, Cary, NC). The authors could not find any gender differences or the effect of body mass on the perceptual levels. Therefore, the data was not normalized by subject weight.

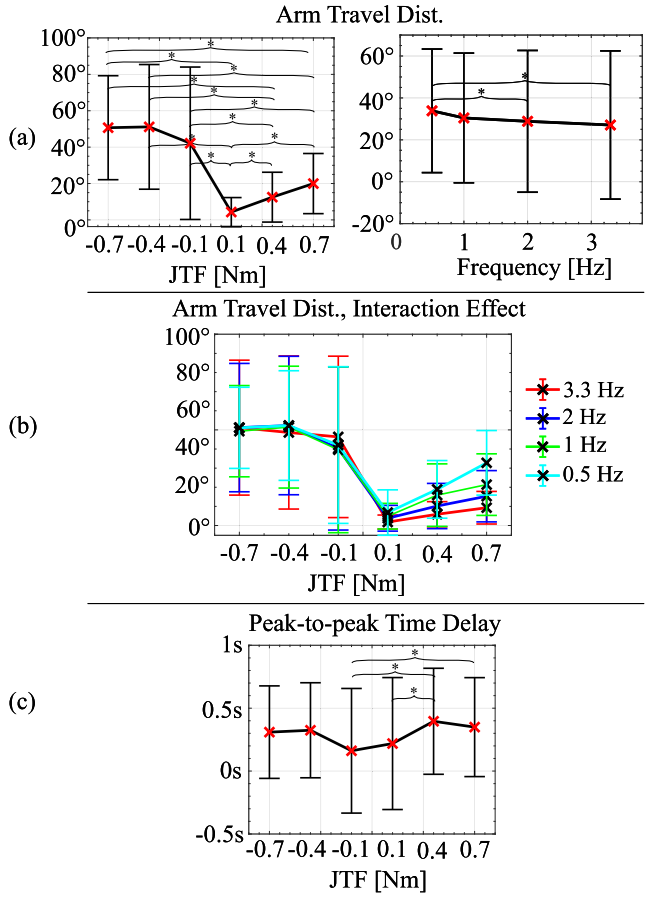

FIGURE 7. Measurements of the tracking data for the Current Pulse. (a): Arm's Traveling distance with JTF (left) and Arm's moving speed (right) as fixed effects. (b): Interaction effect between the magnitude of the JTF and the movement speed on Arm's traveling distance. The arm travel distances plotted are the absolute value of the travel distance for ease of comparing the positive and negative torques; the negative torques resulted in negative travel distances. (c): Peak-to-peak time delay from a Current Pulse. Positive JTF values are flexional inputs; the negative JTF values are extensional feedback. For (a) and (c), the statistically different pairs ($p < 0.05$) are highlighted with asterisks.

A. CURRENT PULSE

The goal of the Current Pulse experiment was to determine the relative effects of the current magnitude and duration in driving the arm's movement. The following equation was used for data processing, for each segment i:

$$\theta_{Current\ Pulse,i} = |\theta_{end\ arm,i} - \theta_{start\ arm,i}|$$

where the $\theta_{end\ arm,i}$ is the arm position at the endpoint of segment i, and $\theta_{start\ arm,i}$ is the arm's position at the beginning of the segment. Figure 5(a) illustrates how the segmentation is performed. Since the current pulse was applied as a double-pulse shape (positive-negative or negative-positive), two peak points were identified. Figure 6(a) shows CP results for the segmented 10 A input.

The RMANOVA was conducted with the current magnitude and duration as the Independent Variables (IVs) and the arm's traveling distance as the Dependent Variable (DV), with the results in Figure 7. Significant results were found for the duration effect ($F(3, 41.81) = 6.747$, $p = 0.001$)

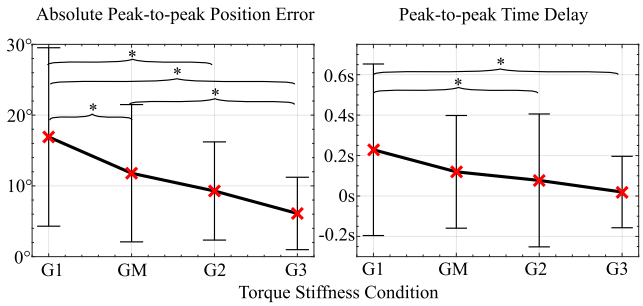

FIGURE 8. Absolute Peak-to-peak Error for Position Pulse for the gain effect (left) and peak-to-peak time delay for the gain effect (right). The significant pairs ($p < 0.05$) are shown with asterisks.

and magnitude effect ($F(5, 60.27) = 115.741,\ p < 0.0001$). Asterisks in Figure 7(a) indicate pairs of conditions that are significantly different.

Significant interactions also occurred with the current magnitude and duration with the JTF applied in the flexional direction (Figure 7(b), positive JTF values). From the pair-wise t-test, the input of 0.74 Nm in the flexional direction has statistical significance between 3.3 and 0.5 Hz ($t = 4.81,\ p = 0.0008$) and between 2 and 0.5 Hz ($t = 3.757,\ p = 0.042$). In comparison, the peak-to-peak time delay only yielded statistical significance for the magnitude ($F(5, 71.23) = 4.107,\ p = 0.0074$), as shown in Figure 7(c).

B. POSITION PULSE

We determined the statistical significance of Position Pulse using the peak-to-peak position error per segment. Figure 5(b) illustrates how the segmentation was performed. Figure 6(b) shows results of the Position Pulse for the segmented 45° input.

Position magnitude, pulse duration, and the torque slope (gain) were selected as the IVs. The DV was the absolute peak-to-peak error per each segment. Significance was found for the gain and duration with a fixed effect test: the gain yielded ($F(3, 12.98) = 19.15, p = 0.0003$) and the duration ($F(4, 22.28) = 3.95, p = 0.034$). The unpooled means and standard deviations of the gain effect are shown in Figure 8(a), with asterisks indicating significantly different pairs. A significant pair for duration was observed between the 1.677 and 0.125 Hz conditions, with results $13.21 \pm 11.92°$ and $8.88 \pm 7.21°$ respectively ($t = 3.419,\ p = 0.0185$). However, we found no significance for the position magnitude between 22.5° and 45°.

The peak-to-peak time delay was also examined with respect to gain, duration, and the input magnitude. A gain effect was found ($F(3, 18.02) = 6.971, p = 0.0182$), shown in Figure 8(b). The duration of the pulse and the magnitude did not have any significance.

We also studied the relationship between the peak JTF applied and the torque stiffness, shown in Figure 9. For the gain effect, the Repeated Measures ANOVA yielded $F(3, 16) = 45.628,\ p < 0.0001$, and the duration effect yielded $F(4, 22.01) = 30.814,\ p < 0.0001$. The interaction effect had a significant effect between gain and duration

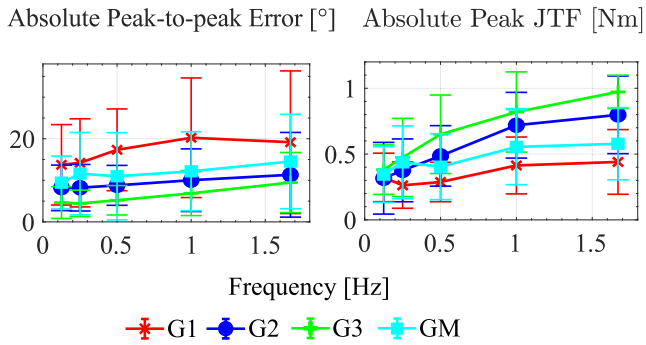

FIGURE 9. Unpooled Means and Stds of Position Pulse, with peak-to-peak position error (left) and peak JTF (right). The means of this data are also plotted in Figure 4 on top of the actual torque stiffness curves, for ease of comparison with them.

TABLE 1. Significant levels of interactions between gain and duration of Position Pulse. The compared DVs are Peak-to-peak position error (left) and peak JTF within the trial (right). A-G are the group labels where the fixed effects with the same label are not statistically significant.

[Hz]	Gain	Position Eror							Peak JTF						
0.125	G1	A	B	C	D	E							F	G
	GM		B	C	D	E	F					E	F	G
	G2			C	D	E	F							G
	G3						F					E	F	G
0.25	G1	A	B	C	D									G
	GM	A	B	C	D	E	F				D	E	F	G
	G2			C	D	E	F					E	F	G
	G3						F				D	E	F	G
0.5	G1	A	B	C										G
	GM	A	B	C	D	E	F					E	F	G
	G2			C	D	E	F			C	D	E	F	G
	G3					E	F		B	C	D			
1	G1	A										E	F	G
	GM	A	B	C	D	E	F			C	D	E	F	
	G2		B	C	D	E	F		B	C				
	G3				D	E	F	A	B					
1.67	G1	A	B								D	E	F	G
	GM	A	B	C	D	E			B	C	D	E		
	G2	A	B	C	D	E	F	A	B					
	G3			C	D	E	F	A						

($F(12, 65.43) = 4.224,\ p < 0.0001$). Table 1 shows the pairs of conditions in Figure 9 that are significantly different.

The test results were also evaluated in the frequency domain: the transfer function of the arm's position to the robot's pre-defined trajectory is shown in Figure 10.

A final set of results for the Position Pulse experiment is shown in Figure 4. There, small ×s indicate the mean error θ_{error} and mean of the peak feedback torque during the experiment, for each gain; ◯s are the means of the ×s for each gain.

C. POSITION STEP

The Position Step was analyzed as the absolute steady-state position error:

$$\theta_{Position\ Step,i} = |\theta_{end\ robot,i} - \theta_{end\ arm,i}|$$

where $\theta_{end\ robot,i}$ is the end position of the desired trajectory for segment i and $\theta_{end\ arm,i}$ is the end position of the arm (as measured by the exoskeleton). Figure 5(c) illustrates how the segmentation was performed. Figure 6(c) shows the

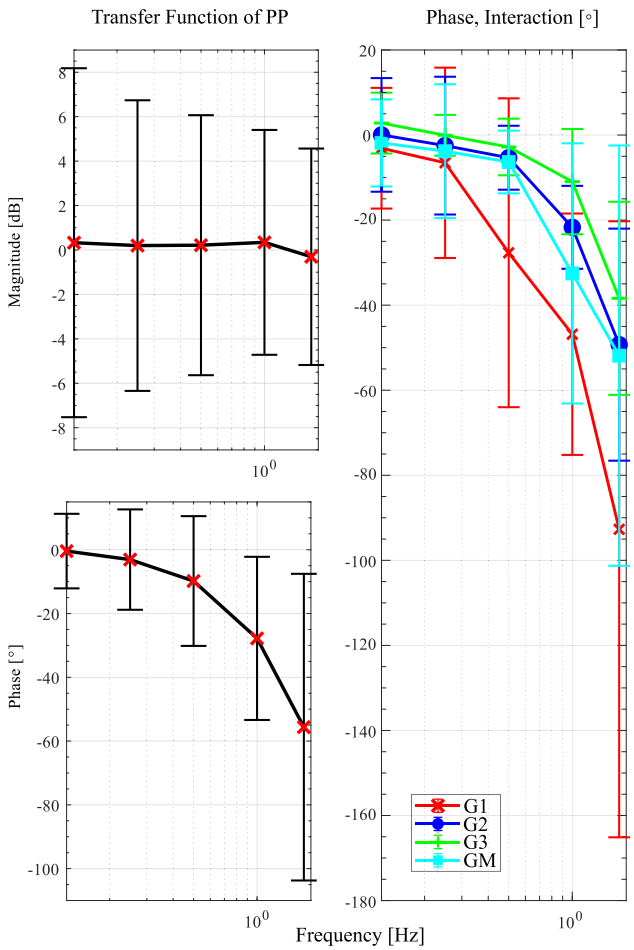

FIGURE 10. Unpooled Means and Stds of the Position Pulse's results, shown in a Bode plot. The magnitude, in dB, is calculated by the ratio of the arm's peak to the input peak. The raised cosine function is treated like a sinusoidal wave when the data was converted into phase. The figure on the right side shows the gain effect on the phase delay.

segmented results for several example Position Step inputs. The fixed effects included gain, absolute position magnitude (i.e., absolute value of the change in arm position), and the arm's movement direction (i.e., flexion or extension). The FDR-corrected p-value for the gain effect is $F(1, 6.241) = 15.198$, $p = 0.035$. The unpooled means and standard deviation are $15.48 \pm 12.44°$ for G1, and $9.04 \pm 9.96°$ for G2. We also found significance between the extensional motion and flexional motion with the FDR correction ($F(1, 7.769) = 11.465$, $p = 0.035$). The detailed means and standard deviations are: $8.95 \pm 7.49°$ for extensional input, while $15.29 \pm 14.00°$ for flexional feedback. However, we did not find significance among the input magnitudes.

In terms of response time, we analyzed the 90% rise time in terms of gain, direction, and magnitude of the step input. G1 was shown to be different from G2: $F(1, 8.65) = 16.685$, $p = 0.021$ (FDR corrected). G1 yielded 0.638 ± 0.434 s while G2 was 0.468 ± 0.296 s. However, no significance was found among the magnitude and directions of the input.

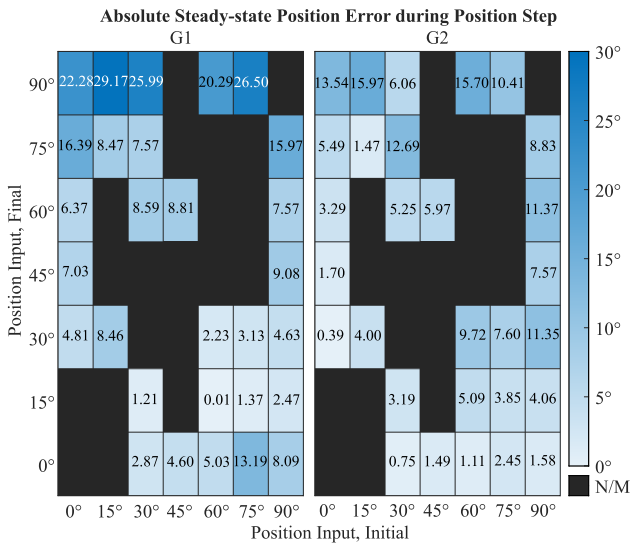

FIGURE 11. Unpooled mean values of steady-state Position Step error represented as a vector table. The x-axis indicates the arm's initial position and the y-axis is the final position. The Left panel is the G1 condition and the Right panel is G2. 0° is where the arm is fully extended. N/M indicates that the corresponding initial-final step input pair was not measured.

Unlike the Position Pulse which always began at 45°, the Position Step had several beginning positions and end positions. Because of this, we could create a mapping between the start and end angles, shown in Figure 11. The values in the figure are the unpooled means.

IV. DISCUSSION

Although both increased magnitude and duration of the pure torque pulse (Current Pulse condition) are responsible for increasing the arm's travel distance (Figure 7(a)), the changes in the arm's travelling distance vary much more with the magnitude than the frequency. In Figure 7(a), the different torque magnitudes lead to arm travel distances ranging from close to 5° (0.1 Nm flexion) to > 50° (-0.4, -0.7 Nm extension) whereas with different frequencies, the arm only travels between 25-35°. Looking at the interaction effect between torque magnitude and frequency in Figure 7(b), the flexional JTF of 0.74 Nm (which is equivalent to the 10 A current) causes different arm traveling distances with different frequencies (durations) of the torque input, and the arm travel distance is roughly proportional to the pulse duration. However, for small input torques of 0.144 Nm, the arm moves roughly 5° regardless of how fast the robot drives the arm. In contrast, the extensional direction of torque inputs leads the arm to move to the end of its range of motion (45°) regardless of the input pulse duration (0.3-2 s) or torque (0.144-0.72 Nm). The results illustrate that people are more sensitive to torques in the extensional direction than flexional direction. It is not entirely clear why this could be, although potentially moving the arm in the flexional direction could be influenced by a higher mechanical joint stiffness as the biceps become compressed. The different behavior in flexion and extension suggests that for motion guidance with JTF (similar to the Position Pulse and Position Step conditions in this

paper), different torque stiffnesses in flexion and extension may lead to optimal tracking behavior.

Interestingly, the input of 2 A current pulse, which is 0.144 Nm, is similar to the smallest noticeable elbow torque with the arm at rest (0.098 − 0.101 Nm) [27], [34]. Even with this barely-noticeable torque, subjects could follow the exoskeleton's guidance to some extent.

However, the peak-to-peak time delay at different arm speeds is indistinguishable with all pulse durations. In terms of the magnitude effect, an almost-symmetric pattern between flexional and extensional torques is shown in Figure 7(c). For the 2 A current input (0.1 Nm), the 0.25 Hz condition resulted in a large standard deviation and a slightly negative peak-to-peak time delay, meaning that the participants reached a maximum before the actual torque did, presumably because they had a hard time detecting the torque. Therefore, it appears that the JND level of torque could be helpful in the initiation of the movement, yet is insufficient for tracking tasks.

While the Current Pulse applied an open-loop torque to the arm, the position controller corrects the arm movement during tracking in the Position Pulse (PP) condition. Thus, the gain level dominates over the other fixed effects of the pulse's duration or magnitude. We hypothesized in the Introduction that once the torque slope becomes so large that $\theta_{threshold}$ becomes θ_{stall}, the tracking performance might be degraded. However, a higher gain led to better accuracy in speed and position even for our steepest gain, G3 (Figure 8). The result contradicts our pilot test, where the subject was guided with a fixed torque of the JND magnitude in either flexion or extension. During the pilot test, subjects were confused about the feedback and could not follow the cues; the tracking behavior was accompanied by overshoot and multiple back-and-forth oscillations. The critical difference between the test result and the pilot test was that the gain G3 still provided angular information during this experiment; indeed, the mean peak torques of 0.4-1 Nm were well above the stationary JND torque of ∼0.1 Nm and JND torque while in motion of ∼0.4 Nm [34] (see Figure 4). It thus appears that the slope of G3 was not steep enough to realize a virtual wall effect with the system.

Another noticeable point is that GM acts as a slope between G1 and G2 despite the fact the slope G1 was applied from $0 - 13°$ of error and G2 for $> 13°$. In terms of both position error and time delay, GM was positioned in between G1 and G2 in most cases (see Figure 8). The tracking performance could be listed as G3-G2-GM-G1 from the most accurate result to the least accurate. That order is completely the reverse of the position to reach the stall torque level (θ_{stall}): 11°(G3)-13°(G2)-27°(GM)-87°(G1). This could imply that the participants perceive the JTF created by the GM as the average of G1 and G2, rather than recognizing the two discrete torque sections. In Figure 4, it can be seen that the conditions with smaller peak torques (×s with $\theta_{error} < 13°$, which is where the gains diverged) gain GM still had higher angular errors than G2. It is likely that while the mean peak torques were below the point where the torque curves diverged, the standard deviations were large, and the small extra torque from G2 above $\theta_{error} = 13°$ made a large impact on subject perceptions in some trials.

Referring to Figures 4 and 9, the steeper gains (e.g. G3) had lower peak-to-peak errors than the shallower gains (e.g. G1). The differences in error were substantial, with G1 having errors around 10° larger than G3 independent of frequency. Even with a peak torque of less than 1 Nm, gain G3 was able to produce tracking errors of less than 10° on average across all frequencies, and errors of around 5° at low frequencies ($\leq$ 0.5°). The low peak torques required for reasonable tracking performance validate this as a good approach for haptic feedback to a person.

Interestingly, at 0.125 Hz, where the arm was moving the slowest, all of the gains had almost exactly the same peak JTF torque, but G3 resulted in better accuracy than G1 (and the other gains were in between the two). Thus, the steeper slope of G3 allowed participants to track the commanded position pulse more precisely. For frequencies higher than 0.125 Hz, it is curious that the steeper gains (e.g. G3) had higher peak torques than the shallower gains (e.g. G1). This is likely due to the masking effect of moving the arm quickly [34]; with G3, the peak-to-peak time delay was much smaller than with G1 (Figure 8): above 0.2 s for G1, but close to 0 s for G3. Thus, people moved to the desired arm position much faster, which would mean they were subject to an increased masking effect due to the arm's velocity. A higher feedback torque was thus required to get the participants to notice their errors. This experiment thus quantifies the trade off between required feedback torque and speed of motion. For applications where the JTF must maximally not disturb the wearer, slow movement speeds are necessary.

We had anticipated that G1 would have 30° of offset larger than GM for situations in which high torques ($>$ 0.5 Nm) were needed because of the difference between the two gain conditions (Figure 4). However, with gain G1 there were very few trials that required torques larger than 0.5 Nm. In the end, the G1 and GM conditions had peak angular errors that were only around 5° different (see Figures 4 and 8). This difference is still less than the angular difference between the torque stiffness curves at 0.3-0.5 Nm (which were the mean peak torques in these conditions), however; this is likely due to the velocity masking effect, where with G1 people were more sensitive to torque cues due to moving more slowly, and thus did not require as large of angular errors to perceive corrective torques as they did with GM.

We examined the frequency elements of the PP with a Bode plot in Figure 10. The magnitude element of the transfer function did not have noticeable changes over the arm speed. However, the phase plot of the PP per different gain shows differences. Previously, kinesthetic guidance was studied with the left arm's position guiding the right arm's movement [20]. Neilson found that around 1 Hz, the phase had a −50° delay. In our test results, gain G1 also had a phase close to −50° at 1 Hz, while G2 and GM had similar phase

values at close to 1.67 Hz. Gain G3 never reached a phase lag of −50° even for the fastest pulses.

Overall, if we treat the arm being driven by the exoskeleton with JTF as a second-order system, the cutoff frequency would occur with a phase delay of −90°. For gain G1, this occurred at around 1.67 Hz, while for the other gains it would occur at higher frequencies than were tested (likely 2-3 Hz). In comparison, Neilson found that the highest closed-loop tracking elbow response (the right arm tracking the left arm) was 2 Hz, while the elbow could produce open-loop oscillations between 4-6 Hz. It thus appears that JTF has a bandwidth similar to, but probably higher frequency than, kinesthetic guidance between arms. It may be that JTF can achieve higher frequencies because the exoskeleton itself may push on the arm a small amount, moving it in the desired direction. Alternatively, the neural response may be somehow faster when haptic feedback is applied to the arm that is moving as compared to the contralateral side.

Similar to the gain effect for the Position Pulse, results from the Position Step (PS) indicate that a higher gain leads to smaller spatial errors and time delays. The arm's step response had a mean 90% rise time of about 0.5-0.6 s depending on the gain, as can be seen in Figure 6, which provides some intuition about how fast a person can follow JTF stimuli.

With the Position Step, we focused on how the tracking performance depended on the motion direction. The directional difference in statistical analysis is illuminated by Figure 11, which shows all of the combinations of input-output positions. The position errors in Figure 11 did not have significant changes over the initial angle (per column). However, they yielded noticeable changes over the final position (per row). The trend was consistent throughout the map that the flexional motion yielded relatively more position error than the extensional motion. For example, this can be seen in Figure 11 where for both G1 and G2 the top row has large position errors (where arm was flexing to end up at 90°). In comparison, the bottom row of both conditions has small values, corresponding to the arm extending to end up at 0°.

One possible reason for these observations is related to the mechanical properties of the elbow joint. According to Latash *et al.*'s study, passive joint stiffness refers to the mechanical properties of body tissues, such as the muscle-tendon complex, and has a property of varying depending on the initial joint position [36]. The author highlighted that passive joint stiffness increases with elbow flexion [36], [38]. Given this, if the exoskeleton is moving the arm and the body is sensing the displacement after the exoskeleton moves it, the exoskeleton will move the arm more in extended positions as compared to flexed positions due to the lower passive stiffness. If the arm moves more, presumably a person would have an easier time sensing that. So, we would expect that extending the arm (and ending up in an extended position) will result in better position tracking accuracy than being guided to flex the arm. However, this is a passive stiffness that occurs when the arm is externally driven, not an active stiffness that occurs while the human is driving their arm, as in this experiment. Therefore, it likely does not entirely explain the differences in position error between the two directions.

Another explanation might be that there is a perceptual difference in direction, meaning that persons perceive flexional or extensional torques differently. In previous work about the JND torques in dynamic conditions [34], flexional torque feedback while the arm was moving in flexion at 200°/s had a higher median value than the extensional torque input while the arm was extending at 200°/s (0.799 and 0.428 Nm, respectively). So, more torque is required to sense flexion torques than extension torques while the arm is moving. In addition, the Current Pulse test (Figure 7) showed that flexional torques drive the arm smaller distances than extensional torques; this too implies that extensional torques are easier to sense. Thus, if the exoskeleton is causing the arm to move in flexion, we would expect the accuracy to be worse than if the exoskeleton was causing the arm to move in extension, which is what was observed in the Position Step results.

V. CONCLUSION

In this study, we explored human tracking performance with respect to torque guidance from an elbow exoskeleton. From the Current Pulse tests, we found that the JND level of torque could initiate tracking motion yet led to poor tracking accuracy. With large torques, there was no statistical difference among time delays even for different frequency pulses. However, the arm responded differently in flexion and extension. Flexion torques led to a travel distance proportional to the torque and varying based on frequency, while extension torque caused the arm to move close to the maximum possible amount for all torques and pulse durations. We next evaluated the position tracking performance of the elbow with JTF under different torque stiffness gains. We did not see a degradation of performance due to a steep torque slope (gain G3); rather, the highest gain was responsible for a higher peak torque during the tracking and better tracking accuracy. In frequency domain, the exoskeleton's kinesthetic guidance with G2 and GM yielded a similar pattern to the kinesthetic guidance via contralateral arm proprioception. Overall, higher velocity motions required higher torques, in accordance with prior observations about the masking effect of moving the arm. Lastly, the torque feedback in the extensional and flexional directions was compared with step inputs. The test results were in agreement with earlier results about the body's response to extensional and flexional torques.

In the future, the implemented torque stiffness in this study (with a linear PD controller) could be improved. Other types of controllers, such as impedance controllers or other functions relating position error to applied torque, could replace the linear slopes tested in this paper and potentially achieve better tracking performance. It would also be interesting to study an optimized torque profile by adopting a higher-level controller. Overall, this study demonstrated that joint torque feedback can be an effective means of kinesthetic motion guidance.

REFERENCES

[1] K. Bark, E. Hyman, F. Tan, E. Cha, S. A. Jax, L. J. Buxbaum, and K. J. Kuchenbecker, "Effects of vibrotactile feedback on human learning of arm motions," *IEEE Trans. Neural Syst. Rehabil. Eng.*, vol. 23, no. 1, pp. 51–63, Jan. 2015.

[2] K. Bark, J. Wheeler, P. Shull, J. Savall, and M. Cutkosky, "Rotational skin stretch feedback: A wearable haptic display for motion," *IEEE Trans. Haptics*, vol. 3, no. 3, pp. 166–176, Jul. 2010.

[3] C. Antfolk, M. D'Alonzo, M. Controzzi, G. Lundborg, B. Rosén, F. Sebelius, and C. Cipriani, "Artificial redirection of sensation from prosthetic fingers to the phantom hand map on transradial amputees: Vibrotactile versus mechanotactile sensory feedback," *IEEE Trans. Neural Syst. Rehabil. Eng.*, vol. 21, no. 1, pp. 112–120, Jan. 2013.

[4] A. W. Shehata, M. Rehani, Z. E. Jassat, and J. S. Hebert, "Mechanotactile sensory feedback improves embodiment of a prosthetic hand during active use," *Frontiers Neurosci.*, vol. 14, p. 263, Mar. 2020.

[5] U. Proske and S. C. Gandevia, "The proprioceptive senses: Their roles in signaling body shape, body position and movement, and muscle force," *Physiol. Rev.*, vol. 92, no. 4, pp. 1651–1697, Oct. 2012.

[6] J. Han, G. Waddington, R. Adams, J. Anson, and Y. Liu, "Assessing proprioception: A critical review of methods," *J. Sport Health Sci.*, vol. 5, no. 1, pp. 80–90, Mar. 2016.

[7] F. M. M. O. Campos and J. M. F. Calado, "Approaches to human arm movement control—A review," *Annu. Rev. Control*, vol. 33, no. 1, pp. 69–77, Apr. 2009.

[8] L. Marchal-Crespo, G. Rauter, D. Wyss, J. von Zitzewitz, and R. Riener, "Synthesis and control of an assistive robotic tennis trainer," in *Proc. 4th IEEE RAS EMBS Int. Conf. Biomed. Robot. Biomechatronics (BioRob)*, Jun. 2012, pp. 355–360.

[9] G. Rauter, R. Sigrist, R. Riener, and P. Wolf, "Learning of temporal and spatial movement aspects: A comparison of four types of haptic control and concurrent visual feedback," *IEEE Trans. Haptics*, vol. 8, no. 4, pp. 421–433, Oct. 2015.

[10] C. Carignan, J. Tang, and S. Roderick, "Development of an exoskeleton haptic interface for virtual task training," in *Proc. IEEE/RSJ Int. Conf. Intell. Robots Syst.*, Oct. 2009, pp. 3697–3702.

[11] N. Thomas, G. Ung, C. McGarvey, and J. D. Brown, "Comparison of vibrotactile and joint-torque feedback in a myoelectric upper-limb prosthesis," *J. NeuroEng. Rehabil.*, vol. 16, no. 1, p. 70, Dec. 2019.

[12] T. Willems, E. Witvrouw, J. Verstuyft, P. Vaes, and D. D. Clercq, "Proprioception and muscle strength in subjects with a history of ankle sprains and chronic instability," *J. Athletic Training*, vol. 37, no. 4, pp. 487–493, Dec. 2002.

[13] R. Larsen, H. Lund, R. Christensen, H. Røgind, B. Danneskiold-Samsøe, and H. Bliddal, "Effect of static stretching of quadriceps and hamstring muscles on knee joint position sense," *Brit. J. Sports Med.*, vol. 39, no. 1, pp. 43–46, 2005.

[14] P. Janwantanakul, M. Magarey, M. Jones, and B. R. Dansie, "Variation in shoulder position sense at mid and extreme range of motion," *Arch. Phys. Med. Rehabil.*, vol. 82, pp. 840–844, Jun. 2001.

[15] S. Gandevia, D. Mccloskey, and D. Burke, "Kinaesthetic signals and muscle contraction," *Trends Neurosci.*, vol. 15, no. 2, pp. 62–65, Feb. 1992.

[16] B. T. Zazulak, T. E. Hewett, N. P. Reeves, B. Goldberg, and J. Cholewicki, "The effects of core proprioception on knee injury: A prospective biomechanical-epidemiological study," *Amer. J. Sports Med.*, vol. 35, no. 3, pp. 368–373, 2007.

[17] K. Yasuda, Y. Sato, N. Iimura, and H. Iwata, "Allocation of attentional resources toward a secondary cognitive task leads to compromised ankle proprioceptive performance in healthy young adults," *Rehabil. Res. Pract.*, vol. 2014, Jan. 2014, Art. no. 170304.

[18] B. D. Beynnon, S. H. Ryder, L. Konradsen, R. J. Johnson, K. Johnson, and A. Renström, "The effect of anterior cruciate ligament trauma and bracing on knee proprioception," *Amer. J. Sports Med.*, vol. 27, no. 2, pp. 150–155, Mar. 1999.

[19] S. M. Lephart, J. J. P. Warner, P. A. Borsa, and F. H. Fu, "Proprioception of the shoulder joint in healthy, unstable, and surgically repaired shoulders," *J. Shoulder Elbow Surg.*, vol. 3, no. 6, pp. 371–380, Nov. 1994.

[20] P. D. Neilson, "Speed of response or bandwidth of voluntary system controlling elbow position in intact man," *Med. Biol. Eng.*, vol. 10, no. 4, pp. 450–459, Jul. 1972.

[21] C. E. Chapman and E. Beauchamp, "Differential controls over tactile detection in humans by motor commands and peripheral reafference," *J. Neurophysiol.*, vol. 96, no. 3, pp. 1664–1675, Sep. 2006.

[22] D. F. Collins, T. Cameron, D. M. Gillard, and A. Prochazka, "Muscular sense is attenuated when humans move," *J. Physiol.*, vol. 508, no. 2, pp. 635–643, 1998.

[23] S. R. Williams and C. E. Chapman, "Time course and magnitude of movement-related gating of tactile detection in humans. III. Effect of motor tasks," *J. Neurophysiol.*, vol. 88, no. 4, pp. 1968–1979, Oct. 2002.

[24] B. Gillespie, M. Modhrain, P. Tang, D. Zaretzky, and C. Pham, "The virtual teacher," in *Proc. ASME Int. Mech. Eng. Conf. Expo.*, Jan. 1998, pp. 171–178.

[25] S. Feyzabadi, S. Straube, M. Folgheraiter, E. A. Kirchner, S. K. Kim, and J. C. Albiez, "Human force discrimination during active arm motion for force feedback design," *IEEE Trans. Haptics*, vol. 6, no. 3, pp. 309–319, Jul./Sep. 2013.

[26] H. Kim and A. T. Asbeck, "An elbow exoskeleton for haptic feedback made with a direct drive hobby motor," *HardwareX*, vol. 8, Oct. 2020, Art. no. e00153.

[27] H. Kim, H. H. Guo, and A. T. Asbeck, "Just noticeable differences for joint torque feedback during static poses," in *Proc. IEEE Int. Conf. Robot. Autom. (ICRA)*, May 2020, pp. 11096–11102.

[28] N. Rehmat, Z. Jie, Q. Liu, S. Q. Xie, H. Liang, and M. Wei, "Upper limb rehabilitation using robotic exoskeleton systems: A systematic review," *Int. J. Intell. Robot. Appl.*, vol. 2, no. 3, pp. 283–295, Sep. 2018.

[29] H. Z. Tan, B. Eberman, M. A. Srinivasan, and B. Cheng, "Human factors for the design of force-reflecting haptic interfaces," *Dyn. Syst. Control*, vol. 55, pp. 353–359, Nov. 1994.

[30] M. O'Malley and M. Goldfarb, "The effect of virtual surface stiffness on the haptic perception of detail," *IEEE/ASME Trans. Mechatronics*, vol. 9, no. 2, pp. 448–454, Jun. 2004.

[31] C. J. Winstein, P. S. Pohl, and R. Lewthwaite, "Effects of physical guidance and knowledge of results on motor learning: Support for the guidance hypothesis," *Res. Quart. Exerc. Sport*, vol. 65, no. 4, pp. 316–323, Dec. 1994.

[32] R. Sigrist, G. Rauter, R. Riener, and P. Wolf, "Augmented visual, auditory, haptic, and multimodal feedback in motor learning: A review," *Psychonomic Bull. Rev.*, vol. 20, no. 1, pp. 21–53, Feb. 2013.

[33] D. J. Reinkensmeyer and M. L. Boninger, "Technologies and combination therapies for enhancing movement training for people with a disability," *J. Neuroeng. Rehabil.*, vol. 9, p. 17, Mar. 2012.

[34] H. Kim and A. T. Asbeck, "Just noticeable differences for elbow joint torque feedback," *Sci. Rep.*, vol. 11, no. 1, Dec. 2021, Art. no. 23553.

[35] M. H. Zadeh, D. Wang, and E. Kubica, "Human factors for designing a haptic interface for interaction with a virtual environment," in *Proc. IEEE Int. Workshop Haptic, Audio Vis. Environ. Games (HAVE)*, Oct. 2007, pp. 21–26.

[36] M. L. Latash and V. M. Zatsiorsky, "Joint stiffness: Myth or reality?" *Hum. Movement Sci.*, vol. 12, no. 6, pp. 653–692, Dec. 1993.

[37] A. J. Kovacs, J. Boyle, N. Grutmatcher, and C. H. Shea, "Coding of on-line and pre-planned movement sequences," *Acta Psychol.*, vol. 133, no. 2, pp. 119–126, Feb. 2010.

[38] W. A. MacKay, D. J. Crammond, H. C. Kwan, and J. T. Murphy, "Measurements of human forearm viscoelasticity," *J. Biomech.*, vol. 19, no. 3, pp. 231–238, Jan. 1986.

HUBERT KIM received the B.S. degree in mechanical engineering from NYU, in 2015, and the Ph.D. degree from Virginia Tech, in 2021. At Virginia Tech, he received an ICTAS Doctoral fellowship. His research interests include human-robot interaction, haptic systems, and wearable robots.

ALAN T. ASBECK received the Ph.D. degree in electrical engineering from Stanford University, in 2010. He is currently an Assistant Professor in mechanical engineering with Virginia Tech, Blacksburg, VA, USA. His current research interests include mechanism design, human-assistance devices, human sensing systems, and robotics.